2013 IEEE/ASME International Conference on
Advanced Intelligent Mechatronics (AIM)
Wollongong, Australia, July 9-12, 2013

Active Robot Hand Compliance using Operational Space and Integral Sliding Mode Control

Jamaludin Jalani[1], Nasiruddin Mahyuddin[2], Guido Herrmann[2] and Chris Melhuish[3]

***Abstract*— This paper establishes a novel approach of robust active compliance control for a robot hand via an Integral Sliding Mode Controller (ISMC). The ISMC allows us to introduce a model reference approach where a virtual mass-spring damper system can be used to design a compliant control. In order to allow for practical grasping, we consider the shape of the object to be grasped. Hence, the work exploits a grasping technique via Cylindrical and Spherical coordinate systems due to their simplicity and geometric suitability. The control uses the operational space approach. Thus, the control is split into a task control and a particular optimizing posture control. The experimental results show that target trajectories can be easily followed by the task control despite the presence of friction and stiction while the posture controller maintains a desired finger posture. When the object is grasped, the compliant control will automatically adjust to a specific compliance level. Once a specific compliance model has been achieved, the fixed compliance controller can be tested for a specific scenario. The experimental results prove that the BERUL hand can automatically and successfully attain different compliancy levels for a particular object via the ISMC.**

I. INTRODUCTION

Emulating the human hand via a robot hand to perform a grasping task can be challenging [1], [2], [3], [4],[5]. One of the functions required by a robot hand is the ability to grasp any objects without damage. For this, a compliant control strategy is important to provide such grasping technique. Some effort has been devoted to realize compliant control [6], [7], [8], [9] based on passive mechanical compliance which is not easily tunable once practically implemented. Different active compliant control strategies have been proposed by [10], [11], [12], [13], [14]. For instance, PD control [15] is one option, although instability may occur (in particular when the hand is in contact with other objects); this might be due to the lack of an accurate model for the robot hand. Hybrid compliance [16], [17] has resolved some of the issues [18, Chapter 9, e.g. pp 397]. The control approach introduces two states [19], [16]. The first state is controlling the positioning error which is also known as controlling an unconstrained mode while the second state is providing force control in a particular direction. Between these two states, there is a transition mode from positioning control to force control. Early controllers resolved this through a switching mode [16] which may be discontinuously achieved. Switching actions may be uncertain and cause instability [20]. More recent solutions have resolved this in a geometric approach, where the directionality expressed by the kinematics Jacobian defines the directions for position and force control [20], [18], [17]. Directional force control approaches are ideal in industrial applications [16], but may be generally problematic in scenarios with humanoid robot hands, where the environment is uncertain and multidirectional (despite exceptions for directional compliance [17]). Thus, robustness to model and environmental uncertainty for compliance control is essential.

In this paper, an integral sliding model control (ISMC) using a model reference idea will be discussed. The reference model will introduce a virtual mass-spring and damper system which will determine the compliant control characteristics, i.e. the ISMC approach is not switching between two different states. ISMC (see [21], [22] for tracking) is a control approach which can counteract system uncertainties and is particularly useful for mechanical systems with stiction and friction. Apart from safely grasping an object through compliance strategies, it is desirable that the robot hand is able to adapt to different compliant levels. This can be realized through the automatic alteration of the above mentioned reference model in an *initial* automatic tuning process of the model parameters.

Providing sufficient knowledge of the object geometry is also an important criterion in order to plan motions and compute successful grasps. Interesting results from [23] can assist researchers to plan their grasping technique. The results show that over 50% of the required grasps are cylindrical, and it is possible for a three-fingered hand to achieve over 90% of these grasps using a cylindrical design approach (see also [24]). Thus, for a suitable grasping geometry, a tested cylindrical coordinate system can be very helpful. In addition, we also suggest a *spherical coordinate system* for objects grasped by the thumb finger. This allows for radial thumb abduction. When touching an object, a human hand does not require very high accuracy. The grasping task needs to guarantee that the fingers sufficiently surround the object, staying in good contact and creating a suitable ergonomics-inspired posture [25]. Thus, the hand grasping may be split into a task where the finger tips touch/grasp the object, while the fingers overall remain in good contact with the object through a suitable finger posture. Hence, a simple way to achieve this desired grasping is by using the operational space approach [26]. In general, the underlying concept is based on the decomposition of the control signal into a task controller and a posture controller. This may have some similarity to the hybrid force/velocity approach of [18, pp.396]. However, the operational space control approach lends itself to a control approach where a high accuracy finger joint trajectory can be avoided. Thus, the main contributions of this paper are

- Introduction of a compliance reference model subject to an external measurement signal to be used via an Integral Sliding Mode Control (this avoids scheduling methods and hybrid compliant control approaches).
- Control of a robot hand via the operational space approach using spherical and cylindrical coordinates.
- Robust finger (i.e. hand) posture optimization via a robust sliding mode posture controller (e.g. [27]) which allows for a practical grasping trajectory and reduces the need for high accuracy.
- Approach for compliant control which is non switching.
- Suggestion of an automatic tuning procedure for the

[1]J. Jalani is now with the Department of Electrical Engineering Technology, Universiti Tun Hussein Onn Malaysia, 86400, Batu Pahat, Johor, Malaysia. He conducted this research work at the Faculty of Engineering, Department of Mechanical Engineering, Univ. of Bristol, BS8 1TR, UK
[2] MN. Mahyuddin and G. Herrmann are with Faculty of Engineering, Department of Mechanical Engineering, University of Bristol, BS8 1TR, UK, mexgh@bris.ac.uk
[3]C. Melhuish is with the Bristol Robotics Laboratory, University of the West of England, Bristol, BS34 8QZ, UK

compliance reference model.

II. Elumotion Hand

Fig. 1 shows the Bristol Elumotion Robot Hand (BERUL). It is to note that all fingers, i.e. index, middle, ring and small finger consist of three links and three joints except the thumb finger. The thumb has four joints and four links. For the majority of the fingers, these joints are connected through a single, flexible pushrod which is then actuated by a leadscrew mechanism that converts a linear movement into a rotary movement for an electrical motor. Nine servo motors have been attached to various fingers of the BERUL hand. In particular, one motor actuator is used for the small and ring finger and two actuators used for the middle, index and thumb finger. Although the middle and index fingers are having two actuators, they follow a planar motion. In contrast, the thumb end effector motion is more complex due to the two applied actuators and their mechanisms: One actuator is used for the push-rod mechanism (i.e. for palmar abduction), while the other motor introduces rotational motion similar to radial abduction. The push rod and leadscrew actuation will create a relational movement of the intermediate and distal phalange links in direct connection to the first (proximal phalange) link of each finger. Measurement of the kinematics of each finger showed that the relationship of the joint movement is sufficiently linear, so that the effect of the pushrod constraining the fingers can be modelled similar to a pulley belt system [28]. This allows a reasonably accurate computation of *the end positions of a each finger tip* via forward kinematics in the targeted spherical/cylindrical coordinate system using the motor position, i.e. the first directly actuated joint angle values of each finger. *For this paper, we focus* on the ring, index and thumb finger, as examples of fingers with one and two actuators with planar and non-planar motion.

III. Cylindrical and Spherical Coordinates

In order to allow for practical grasping for the BERUL fingers, we exploit the cylindrical and the spherical coordinate system. The cylindrical or the spherical coordinate system can be centered at the object to be grasped (see Figure 4 in [29] and Figure 1 for the coordinate system placement. Note that the transformation between Cartesian and Cylindrical/Spherical coordinates follows a standard mathematical calculation.). The cylindrical coordinate system is most suited to the index, middle, ring and small fingers, since these fingers often follow a planar movement, even when they are having several actuators. A thumb generally is more versatile in its movements, as it has to move from its initial position around objects (palmar and radial abduction). Thus spherical coordinates are suited for the thumb. For grasping, it is not necessary to control the joint position of each finger at a high accuracy. Grasping can be easily directed by the radial position r of the finger tip and a preferred posture in case fingers are multi-redundant. Hence, both the cylindrical and spherical coordinates lend themselves to finger control via the radius r.

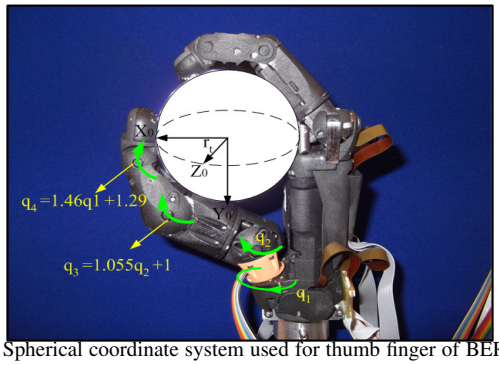

Fig. 1. Spherical coordinate system used for thumb finger of BERUL hand

IV. Controller Structure

The overall structure for active compliance controller for the BERUL fingers is depicted in Figure 2. It has two primary parts: the first part is the ISMC based compliance controller for the task. The second is the posture controller. This is possible as we employ the operational space approach, which allows the geometric splitting into task and posture control.

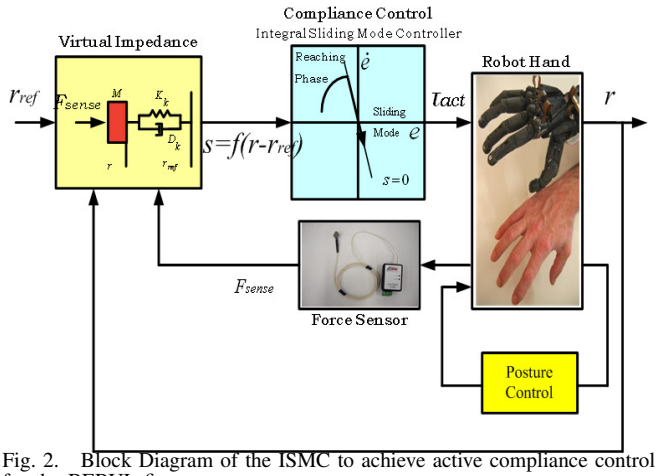

Fig. 2. Block Diagram of the ISMC to achieve active compliance control for the BERUL fingers

A general model of a robot is

$$M(q)\ddot{q} + V(q,\dot{q})\dot{q} + G(q) + D_f = \tau. \quad (1)$$

where M, V and G provide mass, velocity and gravity terms respectively. The vector D_f represents amplitude limited friction and stiction disturbances and uncertainties; in addition, D_f can also represent forces which result from interaction of the hand with other objects. [1] The torque vector τ represents the external actuating torques affecting each joint. This representation certainly holds for each specific finger for which we develop here the controller. It is to point out that in the context of the robot hand, the term $V(q,\dot{q})\dot{q}$ has very little significance. However, the terms $G(q)$ and D_f clearly have significant influence, considering that the practical BERUL hand is to be attached and moved with the robot arm. Moreover, friction and stiction has significant effect due to the pushrod mechanism.

A. Task Control: *Model-reference ISMC for compliance and robustness*

As discussed before, the task coordinate of interest is the radial position r (in the cylindrical/spherical coordinate system), which can be determined by the joint coordinates q. The relevant Jacobian, $J(q)$, of the task coordinate r is defined as

$$J = \frac{\partial r}{\partial q} \quad (2)$$

[1] For control, the forces D_f do not need to be known, as sliding mode control can effectively counteract against them. For active compliance, some of these forces will be measurable to be augmented into the compliance control scheme.

Considering kinematic redundancy of thumb and ring fingers (i.e. the dimension of the task is strictly less than the dimension of the configuration space), the following pseudo inverse as in [30], [31] is used:

$$\bar{J} = M^{-1}J^T(JM^{-1}J^T)^{-1} \tag{3}$$

Thus, using equation (2) allows us to project joint space dynamics (1) into the task space dynamics of the radius r as follows:

$$\bar{M}(q)\ddot{r} + \bar{V}(q,\dot{q})\dot{r} + \bar{G}(q) + \bar{D}_f = F. \tag{4}$$

where $\bar{M}(q) = (JM^{-1}J^T)^{-1}$, $\bar{V} = \bar{J}^TV - M\dot{J}\dot{q}$, $\bar{G} = \bar{J}^TG$ and $F = \bar{J}^TJ$. For control, estimates of all system parameters are needed, i.e. $\hat{\bar{M}}$ is the estimate for $\bar{M}$ while $\hat{\bar{V}}$, $\hat{\bar{G}}$ are the two other respective estimates. Friction and other un-modeled forces are $\bar{D}_f = \bar{J}^TD_f$. A typical feedback linearization controller [18, pp.330] with PD controller is:

$$F_0 = \hat{\bar{M}}(q)f^* + \hat{\bar{V}}(q,\dot{q})\dot{r} + \hat{\bar{G}}(q). \tag{5}$$

where $f^* = \ddot{r}_d(t) + K_pr_e + K_d\dot{r}_e$ and r_e is a radial error defined as $r_e(t) = r_d(t) - r(t)$ with $[r_d(t)\ \dot{r}_d(t)\ \ddot{r}_d(t)]$ being the reference trajectory and its time derivatives. Multiplying J in equation (5), the task space control is obtained as follows.

$$\tau_{task} = J^T(F_0 + F_1) \tag{6}$$

where F_1 is to be defined next: Note that the expression (5) contains an estimate of the finger dynamics. These estimates are generically not easily obtained so that the estimation error with respect to $(\bar{M}\ddot{r}_d + \bar{V}(q,\dot{q})\dot{r} + \bar{G}(q) - \hat{\bar{M}}\ddot{r}_d - \hat{\bar{V}}(q,\dot{q})\dot{r} - \hat{\bar{G}}(q))$ and also the additional forces $\bar{D}_f$ need to be compensated for. Although these errors can be significant, they are in general amplitude bounded. Thus, the task controller, F_0 (6), is now to be augmented by an integral sliding mode controller, F_1, to allow for the required controller robustness and active compliance.

1) Integral Sliding Mode Controller: Now, by using the ISMC approach [21], the task control torque is extended by the nonlinear sliding mode term F_1 (6):

$$F_1 = -\Gamma_0(\frac{s}{\parallel s \parallel + \delta}), \quad \delta > 0, \quad \Gamma_0 > 0. \tag{7}$$

and

$$s = \dot{r}_e + K_sr_e + K_i\int_0^t r_e d\xi - \int_0^t G_fHd\xi - \dot{r}_e(0) - K_sr_e(0) \tag{8}$$

where $r_e(0)$ and $\dot{r}_e(0)$ are initial conditions. Consider that $\int_0^t(\cdot)d\xi$ are integrals over time with integrant ξ. Following the analysis of [21], the sliding mode term enforces $s = 0$ for $\delta \to 0+$ and large enough $\Gamma_0 > 0$, i.e.

$$\Gamma_0 > \left\| (\bar{M} - \hat{\bar{M}})\ddot{r}_d + \bar{V}(q,\dot{q})\dot{r} + \bar{G}(q) - \hat{\bar{V}}(q,\dot{q})\dot{r} - \hat{\bar{G}}(q) + \bar{D}_f \right\| \tag{9}$$

(The scalar $\delta > 0$ is introduced to avoid any possible chattering in the control action due to the nonlinear sliding mode term.) This implies that the following second order dynamics govern for $s = 0$ the robot finger:

$$\ddot{r}_e + K_s\dot{r}_e + K_ir_e = G_fH \tag{10}$$

where G_f is a positive scalar and H is an external force measurement, obtained via specially introduced sensors.[2] K_s is a damping coefficient and K_i is a stiffness coefficient of the reference model. In contrast to former work, the introduction of the external signal into the reference model (10), in particular also for the operational space control context, creates a robust ISMC based compliance control approach.

2) Robustness: The ISMC has been a well investigated control method due to its robustness [32], [33], [34]. Thus, further significant technical detail which proves robustness, in particular (8), is here avoided. It has been shown that ISMC is superior in the context of *trajectory following* for the BERUL hand subjected to friction, in comparison to many other control methods [22], [28].

B. Posture Control For Grasping

The posture controllers are meant to regulate the remaining degree of freedom, which is not controlled by the task controller. The index and the thumb fingers have both two actuators to control their finger tip position in terms of radial position and posture. The idea for the posture is to minimize a cost function, $U(q)$, which guarantees a certain 'optimal' (nominal) positioning of the redundant degrees of freedom. In case of [26] and [27], this was an effort minimizing cost function based on the effects of gravity. This has induced human like motion for a robot torso and arm control. In our case, the effects of gravity are too strongly varying with the hand movement so that a more specific hand posture cost is needed here.

1) Posture Control for Index and Thumb Fingers: We consider the thumb and the index finger which have two actuated degrees of freedom, q_1 and q_2. The geometric projection matrix $N = (I - \bar{J}^T\bar{J}^T)$ is important for the posture task, as it defines the null space of the task controller. (Note that the ring finger discussed here in this paper has only one actuator where all joints are connected through a push rod. For this finger $N = 0$). The overall control signal for a BERUL finger can be written as:

$$\tau = J^T(F_0 + F_1) + N^T(-K_{dp}\dot{q} - K_{SL}\frac{\hat{\bar{M}}\hat{s}}{\parallel \hat{s} \parallel + \delta_{SL}}) \tag{11}$$

where $K_{dp} > 0$, $K_{SL} > 0$ and $\delta > 0$. The variable $\hat{s}$

$$\hat{s} = B(\dot{q} + K_v(\frac{\partial U}{\partial q})^T) \tag{12}$$

introduces a sliding mode variable for the posture control where

$$B = (I - J^T(JJ^T)^{-1}J) \tag{13}$$

The matrix B is a projection matrix similar to N. In the ideal case, the nonlinear sliding mode term enforces $\hat{s} = 0$ for $\delta_{SL} \to 0+$; the posture is therefore robust to system uncertainty [27]. This introduces a gradient descent approach which minmimizes $U(q)$ (additional explanations in [27]).

Instead of using gravity terms to derive the posture controller function [26], [27], a new cost function is given as follows:

$$U(q) = w_1(q_1 - \phi_1)^2 + w_2(q_2 - \phi_2)^2 \tag{14}$$

$w_1 > 0$, $w_2 > 0$, ϕ_1 and ϕ_2 are the choice of the designer for the degrees of freedom to q_1 and q_2 respectively.

Remark 1: The cost function $U(q)$ is to be minimized to guarantee a nominal posture of the thumb and the index finger. Thus, once $U(q) = 0$, the nominal position would be $q_1 = \phi_1$ and $q_2 = \phi_2$. However, the task controller has priority over the posture controller ([26] and [27]). So that the posture cost is not always at its minimum.

[2]In the case of the BERUL hand, we have used *S*ingle-*P*oint *T*actile *S*ensors which allow for force sensing at the BERUL finger tips; see Section VII for further detail.

V. COMPLIANCE CONTROL AND MODEL REFERENCE BEHAVIOR

A. Compliance

For compliance, we reconsider the sliding variable s and its derivative:

$$\dot{s} = \ddot{r}_e + K_s\dot{r}_e + K_i r_e - G_f H \tag{15}$$

When sliding motion is achieved, then $s = 0$ and in particular $\dot{s} = 0$. For $\dot{s} = 0$, the error dynamics are defined by the damping constant K_s, the spring constant K_i and the external force measurement signal H introduced via the input distribution gain G_f, namely

$$\ddot{r}_e + K_s\dot{r}_e + K_i r_e = G_f H \tag{16}$$

This defines a reference model allowing for active compliance control. *This contrasts to the recent use of ISMC, where the sliding mode dynamics generally define a nominal closed loop behavior without external signals. This is an important tool as the controller guarantees a well defined level of compliance despite the high degree of uncertainty and friction in the robot hands.* A virtual demand model for this is

$$\ddot{r}_r = -K_s\dot{r}_r - K_i r_r + G_f H + K_s\dot{r}_d + K_i r_d + \ddot{r}_d. \tag{17}$$

Thus, the joint coordinates r have to follow the virtual demand r_r in the ideal case, given an original demand r_d.

B. A Virtual Mass-Spring Damper Reference

It is noted that from (16) follows

$$\frac{r_e(s)}{H(s)} = \frac{G_f}{s^2 + K_s s + K_i} \tag{18}$$

where $K_s = 2\zeta\omega_n$ and $K_i = {\omega_n}^2$. The scalars ζ and ω_n are damping ratio and natural frequency respectively. Thus, different K_s, K_i and G_f to be used in order to obtain compliance levels.

C. Computation of Compliance Level for an Object

The reference model cannot be arbitrarily determined and it needs to be bespoke, suitably adjusted to the context of the object handled by the robot fingers, in particular when considering the steady state force equilibrium. For this, let us consider the following mass-spring damper system:

$$\ddot{r}_e + \frac{K_{ss}}{m_v}\dot{r}_e + \frac{K_{ii}}{m_v} r_e = \frac{1}{m_v} f \tag{19}$$

where m_v is a virtual mass of the spring, K_{ss} is a virtual damping constant and K_{ii} is a virtual spring constant. By equating equation (19) with equation (16) the following relations are obtained.

$$\frac{K_{ss}}{m_v} = 2\zeta\omega_n = K_s; \quad \frac{K_{ii}}{m_v} = {\omega_n}^2 = K_i; \quad G_f H = \frac{1}{m_v} f \tag{20}$$

where $G_f = \frac{1}{m_v}$, $H = f$, ω_n. The target is now to determine K_{ss}, K_{ii} and m_v via suitable practical tests and design requirements for compliance and transient behavior. We may assume that ζ and ω_n are given to establish a suitable transient behavior, which fixes K_{ss} and K_{ii}. The sensitivity to the measured force is adjusted through the input gain $G_f = \frac{1}{m_v}$.

It is now the aim to find G_f in a semi-automated process. This is to be carried out once, before any serious compliant interaction task, which is to ensure safe interaction after this initial tuning process. The software-implemented process is given as follows.

1) G_f is set to a significantly large initial value which will make the reference model highly sensitive to any external signal H. A task controller is initiated for a constant demand r_d.
2) The finger is controlled via r_d so that it touches the object. For the finger to reach r_d, it would have to penetrate the touched object. This is certainly to be avoided by the compliance controller and an adjusted value r_r (17). The initial large $G_f > 0$ makes the reference model highly sensitive to a touching interaction of the object with the finger. Once the finger has contacted the object, a sensor signal H is measured. Since a constant target value for r_d is set, the sensor signal H is steadily increasing.
3) A level H_{L1} is used to *initiate the tuning process* for G_f. Hence, once the sensor signal H is larger than H_{L1} for a sufficiently long time, the value of G_f is very slowly decreased in an automated fashion. This will make the reference model less sensitive to H and force r_r to be closer to r_d (17).
4) Once the force sensor signal, H, has surpassed a level H_{L2}, ($H_{L2} \geq H_{L1}$) the decreasing value of G_f is kept fixed. Hence, the choice H_{L2} *defines the maximum force applied to the object and therefore determines the compliance level of the reference model* via the fixed parameters K_s, K_i and G_f. These values are now available for further use.

In summary, the process above allows to introduce a compliancy reference model for a specific object-finger force interaction level H_{L2} in a semi-automated manner. This is to be carried out once for the reference model to be used later for the specific class of object in robot-object interaction.

VI. EXPERIMENTAL SETUP

As a real-time interface, the dSPACE DS1006 Controller Board is used to interact with the BERUL fingers. MATLAB/Simulink models can be compiled easily to real-time code which makes it possible to implement new ideas rapidly. The advantages of using dSPACE are that it is easy-to-use real-time hardware, providing simple and practical graphical programming. The I/O interfaces are conveniently connected via Real-Time Interface blocks for seamless integration into MATLAB/Simulink.

VII. RESULTS

The results are divided into three different cases. Case 1 investigates the effectiveness of the posture controller. Case 2 is for tracking performance. Case 3 shows the performance for different compliance levels for a specific object.

The *S*ingle-*P*oint *T*actile *S*ensors (SPTS) which is mounted on the fingers in particular for the thumb, the index and the ring fingers are used to measure various grasped objects. Thus, only 3 fingers have been tested namely ring, index and thumb finger for practicality and also due to availability of SPTSs (It is not unusual to use three finger hands for practical grasping [23]). The SPTS has a diameter of 1 cm and it has a non-linear pressure output voltage relationship which can be approximated to about 1379 Pa = 2 psi per 1 V. Considering the area of the sensor this relates to 4.33 N per 1 V across the pad of the SPTS. The SPTS uses capacitive-based conformable pressure sensors to accurately and reliably quantify applied forces. The analog voltage outputs are fed back into the controller for force measurement to be used for H (8).

A. Posture Controller Parameters and Results - Case 1

The gains used for the posture controller in particular for the index finger are $K_{dp} = 2$, $K_{SL} = 16$, $K_v = 4$, $w_1 = 3$ and $w_2 = 3$. The nominal link positions ϕ_1 and ϕ_2 are chosen as $\phi_1 = 0.45rad$ and $\phi_2 = 1.5rad$. This in fact defines a finger in a slightly bent, almost-open hand position. Thus, once the task controller is enabled (task control has priority over posture), the nominal "almost-open" finger posture (following ergonomics studies in [25]) will guarantee that the finger encloses the object. On the other hand, the gains for the thumb finger are $K_{dp} = 2$, $K_{SL} = 160$, $K_v = 4$, $w_1 = 2$ and $w_2 = 2$. The nominal positions of the thumb are $\phi_1 = -2.5rad$ and $\phi_2 = 1.5rad$. They enforce for the thumb finger to move from an initial (open hand) position to a position (Figure 3, subfigure 1) where the thumb is in front of the object (Figure 3, subfigure 6). Hence, although the task controller has priority to achieve the correct *radial finger tip position*, the posture controller guarantees that the redundant degrees of freedom of the hand permit practical, ergonomics-based grasping positions [25], which is not achievable via task control only.

B. Reference Model Parameters

Using (16), the reference model parameters have been chosen as follows: $K_s = 8$ and $K_i = 18$ which implies $\omega_n = 4$ and $\zeta = 0.9$. The choice of $\omega_n = 4$ and $\zeta = 0.9$ will guarantee an approximate settling time for 1 second for a critically damped reference model.

C. Tracking Results - Case 2

The results show that, while maintaining a desired posture motion as depicted in Figure 3, the tracking of r can be achieved (see Figure 4). Moreover, the results also show that the fingers satisfactorily follow a desired trajectory (i.e. r follows r_d) during opening and the grasping period. More specifically, the task controller performance is still very good despite the posture controller forces the index finger to retain an "open" finger position as much as possible. The thumb finger moves to the last position as nominally desired (see Figure 3, subfigures 1-6). Thus, the posture controller guarantees that the fingers do not collide with the touched object. The space operational approach creates a seemingly natural appearance.

D. Compliance level results for an object - Case 3

We have investigated two different options for the permissible contact forces H_{L2} for grasping a *hard* rubber ball. The level $H_{L2} = 0.01\ V(0.0433\ N)$ and later $H_{L2} = 0.04\ V(0.1733\ N)$. These force levels are chosen to enable object grasping without damaging the object (and also the robot hand). The lower force $H_{L2} = 0.01\ V(0.0433\ N)$ permits a very light grasp, just avoiding object slippage.

The results reveal that a suitable reference model for both H_{L2} can be satisfactorily achieved for both levels as shown in Figure 5 and Figure 6 within the first 10 seconds. It shows that different levels of compliance are feasible for the same object. Moreover, the suggested technique to capture an appropriate G_f is reliable since it can be repeated.

Moreover, in Figure 5 and Figure 6, the compliance control action for fixed $G_f = const.$, $G_f > 0$, is assessed. This can be seen after a period of 60 seconds. Note that during the period from 40 seconds to 60 seconds the fingers are open (i.e. not grasping).

It is also visible, in particular for the ring finger that the pressures exerted on the object must be higher for $H_{L2} = 0.04\ V(0.1733\ N)$ in contrast to $H_{L2} = 0.01V(0.0433\ N)$ since r_d and r_r are slightly closer together. Generally, the gain G_f is smaller for $H_{L2} = 0.01\ V(0.0433\ N)$ in relation to $H_{L2} = 0.04\ V(0.1733\ N)$ (see Tables I and II). Note the rather nonlinear relationship between H_{L2} and G_f for the two options. The decrease of G_f from $H_{L2} = 0.01\ V(0.0433\ N)$ to $H_{L2} = 0.04\ V(0.1733\ N)$ appears to be small, but is was found to be a repeatable result. The small difference in G_f for $H_{L2} = 0.04V(0.1733\ N)$ and $H_{L2} = 0.01V(0.0433\ N)$ may be explained by the material properties of the touched object.

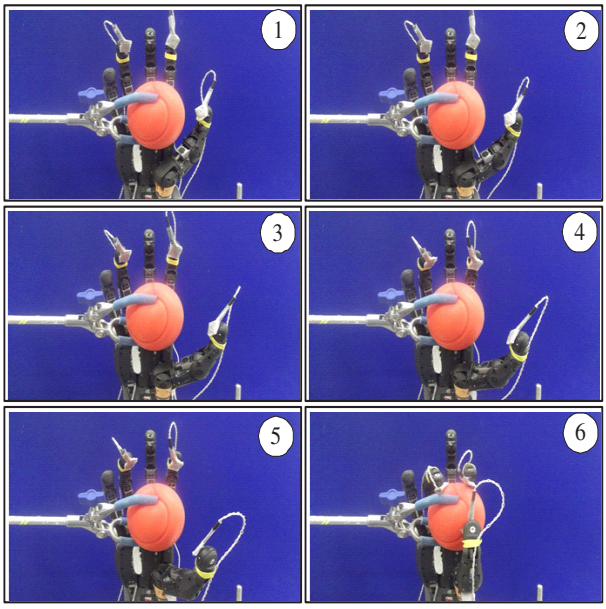

Fig. 3. Cylindrical orientation for index and ring fingers while spherical motion for thumb finger

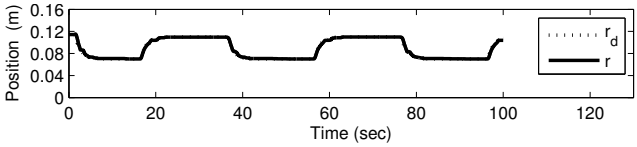

Fig. 4. r_d-tracking for thumb finger in Spherical coordinates

TABLE I

DESIRED FORCE FOR LEVEL 0.0433 N (0.01V)- HARD RUBBER BALL

Finger	G_f	H_{L2} (V)
Thumb	9.519	0.01
Index	9.959	0.01
Ring	9.993	0.01

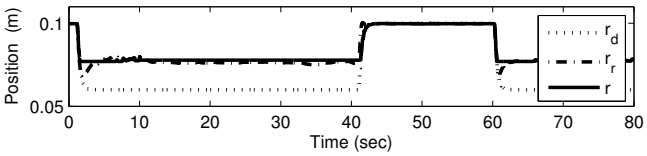

Fig. 5. Compliance performance for level 0.0433 N (0.01V)

TABLE II

DESIRED FORCE FOR LEVEL 0.1733N (0.04V) - HARD RUBBER BALL

Finger	G_f	H_{L2} (V)
Thumb	8.349	0.04
Index	9.851	0.04
Ring	9.118	0.04

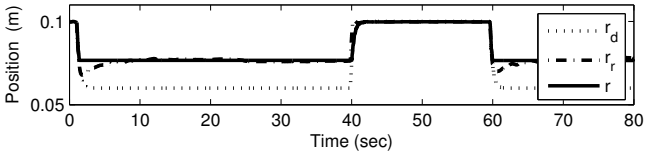

Fig. 6. Compliance performance for level 0.1733 N (0.04V)

VIII. CONCLUSION

In this paper, we propose a novel approach for active compliance control via Integral Sliding Mode Control (ISMC). The ISMC allows us to introduce a model reference approach where a virtual mass-spring damper can be used to design a compliant control. The finger motion is controlled by a posture controller and a task controller as parts of an operational space controller. Both controllers use sliding mode methods to ensure robustness. Results show that the task controller can achieve indeed good tracking performance despite high levels of stiction and friction. The idea of using cylindrical and spherical coordinates and the posture controller of the index and thumb finger guarantees that both fingers move around the touched object without collision and it gives priority to the grasping task. This will allow for practical grasping via the chosen geometry.

The tactile pressure sensors are mounted on the BERUL fingers to permit only a desired force level to affect any object. The effectiveness of the compliant control when grasping similar object has been successfully demonstrated at different desired force levels via an automated tuning procedure. The automated tuning process has shown that reference models for particular force levels can be easily achieved. It shows that higher desired forces require a 'stiffer' reference model. The method is also suitable for achieving compliance levels for different objects, as demonstrated in additional studies (These studies are not included in this paper due to space reasons).

ACKNOWLEDGMENT

The CHRIS (Cooperative Human Robot Interaction Systems) project is funded by the European Commission's Seventh Framework Programme (FP7) and will run from 2008-2012. This research is also partially funded by the Malaysian Government.

REFERENCES

[1] S. Jacobsen, J. Wood, D. Knutti, and K. Biggers, "The utah/m.i.t. dextrous hand: Work in progress," vol. 3, no. 4, pp. 21–50, 1984.

[2] ShadowRobot, "Design of a dextrous hand for advanced clawar applications," in *In Proceedings of CLAWAR*, 2003, pp. 691–698.

[3] M. Grebenstein, A. Albu-Schaffer, T. Bahls, M. Chalon, O. Eiberger, W. Friedl, R. Gruber, S. Haddadin, U. Hagn, R. Haslinger, H. Hoppner, S. Jorg, M. Nickl, A. Nothhelfer, F. Petit, J. Reill, N. Seitz, T. Wimbock, S. Wolf, T. Wusthoff, and G. Hirzinger, "The dlr hand arm system," in *Robotics and Automation (ICRA), 2011 IEEE International Conference on*, may 2011, pp. 3175 –3182.

[4] C. Borst, M. Fischer, S. Haidacher, H. Liu, and G. Hirzinger, "Dlr hand ii: experiments and experience with an anthropomorphic hand," in *Robotics and Automation, 2003. Proceedings. ICRA '03. IEEE International Conference on*, vol. 1, Sept. 2003, pp. 702–707.

[5] J. Vandeweghe, M.Rogers, M.Weissert, and Y. Matsuoka, "The act hand: Design of the skeletal structure," in *Proceedings of the 2004 IEEE International Conference on Robotics and Automation (ICRA '04)*, May 2004.

[6] M. R. Cutkosky, *Robotic Grasping and Fine Manipulation*. Norwell, MA, USA: Kluwer Academic Publishers, 1985.

[7] K. L. Johnson, *Contact Mechanics*. Cambridge, UK: Cambridge University Press, Cambridge, 1985.

[8] K. Shimoga and A. Goldenberg, "Soft robotic fingertips," *The International Journal of Robotics Research*, vol. 15, no. 4, pp. 320–334, 1996.

[9] L. Biagiotti, C. Melchiorri, P. Tiezzi, and G. Vassura, "Modelling and identification of soft pads for robotic hands," in *IEEE/RSJ International Conference on Intelligent Robots and Systems (IROS)*, 2005.

[10] H. Liu and G. Hirzinger, "Cartesian impedance control for the dlr hand," in *Intelligent Robots and Systems, 1999. IROS '99.*, 1999.

[11] A. Kugi, C. Ott, A. Albu-Schaffer, and G. Hirzinger, "On the passivity-based impedance control of flexible joint robots," *IEEE Transactions on Robotics,*, vol. 24, no. 2, pp. 416 –429, 2008.

[12] A. Albu-Schaffer, C. Ott, and G. Hirzinger, "A unified passivity-based control framework for position, torque and impedance control of flexible joint robots," *The International Journal of Robotics Research*, vol. 26, no. 1, pp. 23–39, 2007.

[13] S. Khan, G. Herrmann, A. G., Pipe, and C. Melhuish, "Safe adaptive compliance control of a humanoid robotic arm with anti-windup compensation and posture control," *International Journal of Social Robotics*, vol. 2, no. 3, pp. 305–319, 2010.

[14] Z. Chen, N. Lii, T. Wimboeck, S. Fan, M. Jin, C. Borst, and H. Liu, "Experimental study on impedance control for the five-finger dexterous robot hand dlr-hit ii," in *Intelligent Robots and Systems (IROS), 2010 IEEE/RSJ International Conference on*, 2010, pp. 5867 –5874.

[15] P. Tomei, "Adaptive pd controller for robot manipulators," *Robotics and Automation, IEEE Transactions on*, vol. 7, no. 4, pp. 565 –570, aug 1991.

[16] A. Jaura, M. Osman, and N. Krouglicof, "Hybrid compliance control for intelligent assembly in a robot work cell," *International Journal of Production Research*, vol. 36, no. 9, pp. 2573–2583, 1998.

[17] K. Mouri, K. Terashima, P. Minyong, H. Kitagawa, and T. Miyoshi, "Identification and hybrid impedance control of human skin muscle by multi-fingered robot hand," in *IROS 2007. IEEE/RSJ International Conference on Intelligent Robots and Systems, 2007.*, 2007, pp. 2895 –2900.

[18] B. Siciliano, L. Sciavicco, L. Villani, and G. Oriolo, *Robotics: Modelling, Planning and Control*. Springer, 2008.

[19] Y. Xu and R. Paul, "On position compensation and force control stability of a robot with a compliant wrist," in *Robotics and Automation, 1988. Proceedings., 1988 IEEE International Conference on*, vol. 2, April 1988, pp. 1173 –1178 vol.2.

[20] B.-H. Kim, S.-R. Oh, I. Suh, and g.-J. Yi, "A compliance control strategy for robot manipulators under unknown environment," *KSME International Journal*, vol. 14, pp. 1081–1088, 2000.

[21] J. Shi, H. Liu, and N. Bajcinca, "Robust control of robotic manipulators based on integral sliding mode," *International Journal of Control*, vol. 81, pp. 1537–1548 vol.81, 2008.

[22] J. Jalani, G. Herrmann, and C. Melhuish, "Underactuated fingers controlled by robust and adaptive trajectory following methods," *International Journal of Systems Science*, 2012.

[23] D. Akin, C. Carignan, and A. Foster, "Development of a four-fingered dexterous robot end effector for space operations," in *IEEE International Conference on Robotics and Automation*, 2002.

[24] T. Geng, M. Lee, and M. Hlse, "Transferring human grasping synergies to a robot," *Mechatronics*, vol. 21, no. 1, pp. 272 – 284, 2011.

[25] S. C. Bae, "Investigation of hand posture during reach and grasp for ergonomic applications," Doctor of Philosophy, University of Michigan, 2011.

[26] V. DeSapio, J. Warren, O. Khatib, and S. Delp, "Simulating the task-level control of human motion: a methodology and framework for implementation." *The Visual Computer*, pp. 289–302, 2005.

[27] A. Spiers, G. Herrmann, and C. Melhuish, "An optimal sliding mode controller applied to human motion synthesis with robotic implementation," in *American Control Conference (ACC)*, 30 2010-July 2 2010, pp. 991 –996.

[28] J. Jalani, G. Herrmann, and C. Melhuish, "Robust trajectory following for underactuated robot fingers," in *UKACC International Conference on CONTROL 2010*, September 2010, pp. 495–500.

[29] ——, "Robust active compliance control for practical grasping of a cylindrical object via a multifingered robot hand," in *IEEE International Conference on Robotics, Automation and Mechatronics (RAM)*, September 2011.

[30] O. Khatib, "A unified approach for motion and force control of robot manipulators: The operational space formulation," *IEEE Journal of Robotics and Automation*, vol. 3, no. 1, pp. 43 –53, february 1987.

[31] ——, "Inertial properties in robotic manipulation: An object-level framework," *The International Journal of Robotics Research*, vol. 14, no. 1, pp. 19–36, 1995.

[32] M. Yokoyama, G.-N. Kim, and M. Tsuchiya, "Integral Sliding Mode Control with Anti-windup Compensation and Its Application to a Power Assist System," *Journal of Vibration and Control*, vol. 16, no. 4, pp. 503–512, 2010.

[33] M. Defoort, T. Floquet, A. Kokosy, and W. Perruquetti, "Integral sliding mode control for trajectory tracking of a unicycle type mobile robot," *Integr. Comput.-Aided Eng.*, vol. 13, no. 3, pp. 277–288, 2006.

[34] I. Eker and S. Akinal, "Sliding mode control with integral augmented sliding surface: design and experimental application to an electromechanical system," *Electrical Engineering (Archiv fur Elektrotechnik)*, vol. 90, no. 3, pp. 189–197, 2008.